Mechanics of Advanced Materials and Structures

ISSN: 1537-6494 (Print) 1537-6532 (Online) Journal homepage: https://www.tandfonline.com/loi/umcm20

Nonlinear vibration control of a tall structure with tuned liquid column damper

Shueei-Muh Lin

To cite this article: Shueei-Muh Lin (2016) Nonlinear vibration control of a tall structure with tuned liquid column damper, Mechanics of Advanced Materials and Structures, 23:2, 146-155, DOI: 10.1080/15376494.2014.949920

To link to this article: https://doi.org/10.1080/15376494.2014.949920

Accepted author version posted online: 01 Apr 2015.
Published online: 29 Sep 2015.

MECHANICS OF ADVANCED MATERIALS AND STRUCTURES
2016, VOL. 23, NO. 2, 146–155
http://dx.doi.org/10.1080/15376494.2014.949920

Taylor & Francis
Taylor & Francis Group

ORIGINAL ARTICLE

Nonlinear vibration control of a tall structure with tuned liquid column damper

Shueei-Muh Lin

Mechanical Engineering Department, Kun Shan University, Tainan, Taiwan, Republic of China

ABSTRACT

The nonlinear vibration model of a structure with the tuned liquid column damper (TLCD) is established. TLCD is a successful structure control device. The damping of TLCD is amplitude-dependent and consequently nonlinear. Due to its complexity, the effective linear model is considered for investigating structure characteristics in almost all literatures. Moreover, the structure is usually modeled as a single degree of freedom model. However, the analytical solution for this nonlinear system is derived here. Further, it is found that the optimum design of TLCD for the suppression of vibration depends greatly on the structure parameters.

ARTICLE HISTORY
Received 3 January 2012
Accepted 3 September 2013

KEYWORDS
tuned liquid column damper; nonlinear vibration; analytical solution

1. Introduction

In general, high-strength and light-weight materials have widely been used in the construction of high-rise buildings. These structures generally are flexible and susceptible to vibration problems due to earthquake and wind loads. Therefore, controlling devices, passive as well as active, have been developed to suppress structural vibrations.

On behalf of the passive control, a tuned-mass damper (TMD) is widely used to control vibrations in civil engineering structures [1–3]. TMD is a vibration absorber consisting of a mass–spring–dashpot system attached to a structure. Although, TMD is effective in reducing vibrations caused by stationary excitation forces, their performance to suppress seismic response are relatively limited. In addition to conventional TMD, the tuned liquid column damper (TLCD) utilizing water sloshing motion to suppress the vibration is particularly suited for tall building structures. The damper can serve as a vibration absorber during a severe wind or earthquake attack, and as a water storage facility at the top of building structures for daily use. Due to its simple way of adjusting damper parameters, TLCD has definite advantages over other types of vibration absorbers. The TLCD is a passive control device that consists of tube-like containers filled with liquid, preferably water. In motion the fluid oscillates in TLCD. When the fluid flows through the orifice in the horizontal channel, the pressure loss and the damping force will occur. The damping force is usually described as the product of the damping coefficient and the flow velocity. However, the damping coefficient is velocity-dependent and the damping force is nonlinear. Due to its complexity, the effective linear model is considered for investigating structure characteristics [4–15]. Moreover, Wang et al. [8] established a mathematical model of the devised MR-TLCD by using the parallel-plate theory and developed the structure control method incorporating semi-active MR-TLCD by means of the equivalent linearization technique. Lee et al. [13] investigated the identification of a tuned liquid column and sloshing damper (TLCSD). The analytical dynamics of TLCSD was derived from the equivalent linearized TMD model. In general, two kinds of equivalent linearized TLCD models are presented: (1) the minimum error model of damping force [14], and (2) the equivalent energy dissipation model in harmonic motion [15]. In practicality, the coefficient increases greatly with the flow velocity. Therefore, the first effective linear model is not suitable for large velocity. On the other hand, because the damping coefficient of the second model depends on the amplitude of oscillation, it is not suitable for the transient motion.

Because the mathematical model of a tall structure with TLCD is nonlinear and described in partial differential equations, this system is very difficult to solve directly. A lot of literatures approximated this system by linear single degree of freedom model. Moreover, Colwell and Basu [11] investigated the structure control of turbine tower by using TLCD. The turbine tower was modeled as a multi-degree-of-freedom (MDOF) structure.

In this study, the nonlinear vibration model of structure with TLCD is established. The analytical solutions for these nonlinear models of a distributed system governed by partial differential equations are derived. The influences of several parameters on suppressing vibration are investigated.

2. Equation of motion

Consider a tall structure with TLCD, as shown in Figure 1. This structure is excited by an earthquake and the vibration suppression depends on the damping effect of TLCD. Their equations of motion are presented here.

2.1. *Tuned liquid column damper*

Three kinds of TLCD are presented here: (1) The flow channel is uniform and open as shown in Figure 1b. (2) The flow channel

CONTACT Shueei-Muh Lin smlin45@gmail.com Mechanical Engineering Department, Kun Shan University, No. 195, Kun-Da Road, Yong-Kang District, Tainan, Taiwan 710-03, Republic of China

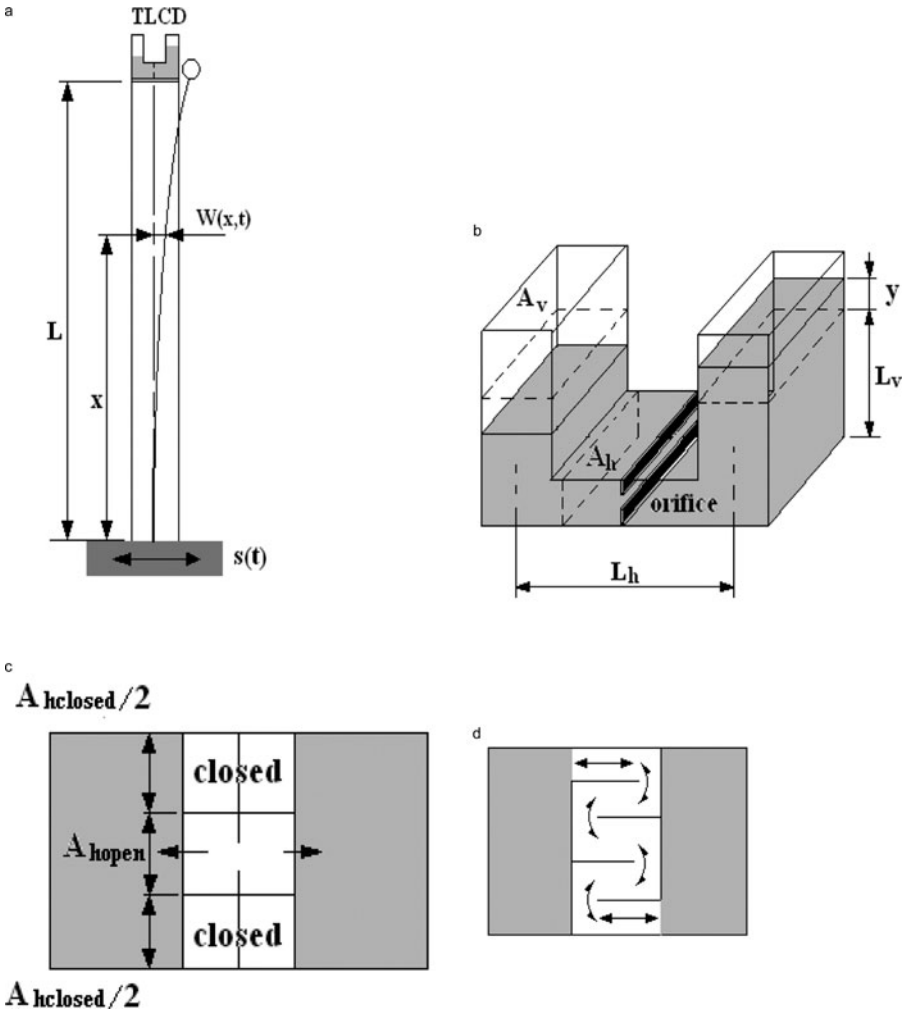

Figure 1. (a) Geometry and coordinate system of a tall building with TLCD. (b) Geometry and coordinate of TLCD. (c) Geometry of partly closed flow channel. (d) Geometry of in-series connecting flow channel.

is partly closed and shown in Figure 1c. (3) The flow channel is in series connection as shown in Figure 1d. The first equation of motion of TLCD is derived by Wu et al. [10]:

$$L_e\ddot{y} + \frac{1}{2}c_\eta r\,|\dot{y}|\,\dot{y} + 2gy = -L_h\ddot{W}(L,t), \tag{1}$$

where y is the change in elevation of the liquid column. $W(L,t)$ is the horizontal displacement of the top of the structure where the TLCD is installed. L_h and L_v are the horizontal and vertical column lengths. A_h and A_v are the cross-sectional areas in the horizontal channel and vertical column, respectively. Further, g is the acceleration due to gravity and $r = A_v/A_h$ is the cross-sectional ratio. $L_e = 2L_v + rL_h$ is defined as the effective length and c_η is head loss coefficient. The damping effect is mainly induced by the flow passing through the orifice.

Obviously, if the damping effect and the forcing term are neglected, Eq. (1) leads to:

$$L_e\ddot{y} + 2gy = 0. \tag{2}$$

Based on Eq. (2), the corresponding natural frequency of TLCD is obtained:

$$\Omega_d = \sqrt{\frac{2g}{L_e}}. \tag{3}$$

Moreover, the derivations of two other equations of motion are listed in Appendices A and B. The equation of motion is the same as Eq. (1) with different definitions of some parameters. Based on Eq. (3), increasing the effective length decreases the natural frequency of TLCD. Further, Appendix A demonstrates that because the area of horizontal channel is reduced, the effective length is increased and the natural frequency of TLCD is decreased. Appendix B also shows that the effective length is greatly increased and the natural frequency of TLCD is decreased significantly.

In terms of the following dimensionless quantities:

$$\bar{g} = \frac{\rho AL^3}{EI}g,\ \bar{L}_h = \frac{L_h}{L},\ \bar{L}_e = \frac{L_e}{L},$$
$$\bar{L}_v = \frac{L_v}{L},\ \bar{y} = \frac{y}{L},\ \xi = \frac{x}{L},$$
$$\tau = \frac{t}{L^2}\sqrt{\frac{EI}{\rho A}},\ w(\xi,\tau) = \frac{W(x,t)}{L},\ \omega_d = \sqrt{\frac{2\bar{g}}{\bar{L}_e}} = \Omega_d L^2\sqrt{\frac{\rho A}{EI}}. \tag{4}$$

The dimensionless equation of motion of the TLCD is:

$$\bar{L}_e\frac{d^2\bar{y}}{d\tau^2} + \frac{1}{2}c_\eta r\left|\frac{d\bar{y}}{d\tau}\right|\frac{d\bar{y}}{d\tau} + 2\bar{g}\bar{y} = -\bar{L}_h\frac{d^2w(1,\tau)}{d\tau^2}. \tag{5}$$

2.2. *Tall structure subjected to base excitation*

Without loss of generality, the tall structure is modeled as a uniform Bernoulli–Euler beam with TLCD. The governing differential equation of the system is:

$$EI\frac{\partial^4 W}{\partial x^4}+\rho A\frac{\partial^2 W}{\partial t^2}=0, \tag{6}$$

at $x=0$:

$$\frac{\partial W}{\partial x}=0, \tag{7}$$

$$W=S(t), \tag{8}$$

at $x=L$:

$$\frac{\partial^2 W}{\partial x^2}=0, \tag{9}$$

$$-EI\frac{\partial^3 W}{\partial x^3}+M_{TLCD}\frac{\partial^2 W}{\partial t^2}+M_h r\frac{d^2 y}{dt^2}=0, \tag{10}$$

where x is the coordinate along the beam, t is the time variable and L is the length of the beam. I and A denote the area moment of inertia and the cross sectional area, respectively. $\rho(x)$ is the mass density per unit volume. M_{TLCD} and M_h are the total mass and the mass of the horizontal part of TLCD, respectively. $S(t)$ is the base displacement due to earthquake. The last two terms of Eq. (10) are the horizontal forces applying to the TLCD.

In terms of the dimensionless quantities (4) and

$$s(\tau)=\frac{S(t)}{L}, \tag{11}$$

the two coupled dimensionless governing differential equations of the system are:

$$\frac{\partial^4 w}{\partial \xi^4}+\frac{\partial^2 w}{\partial \tau^2}=0, \tag{12}$$

at $\xi=0$:

$$\frac{\partial w}{\partial \xi}=0, \tag{13}$$

$$w=s(\tau), \tag{14}$$

at $\xi=1$:

$$\frac{\partial^2 w}{\partial \xi^2}=0, \tag{15}$$

$$-\frac{\partial^3 w}{\partial \xi^3}+m_{TLCD}\frac{\partial^2 w}{\partial \tau^2}+m_h r\frac{d^2\bar{y}}{d\tau^2}=0. \tag{16}$$

3. Solution method

3.1. *Transformed system*

Assume the harmonic motion of liquid in the TLCD:

$$\bar{y}=y_0\sin\omega\tau, \tag{17}$$

where $\omega=\Omega L^2\sqrt{\rho A/EI}$, in which Ω is the frequency of liquid oscillation. The corresponding harmonic solution of the beam is:

$$\begin{aligned} w(\xi,\tau)&=\sum_{n=1}^{\infty} w_{sn}(\xi)\sin n\omega\tau+w_{cn}(\xi)\cos n\omega\tau\\ &=\sum_{n=1}^{\infty} w_{dn}(\xi)\sin(n\omega\tau+\theta_n) \end{aligned} \tag{18}$$

where $w_{dn}=\sqrt{w_{sn}^2+w_{cn}^2}$ and $\theta_n=\tan^{-1}(w_{sn}/w_{cn})$. The corresponding base excitation is:

$$s(\tau)=\sum_{n=1}^{\infty} w_{sn0}\sin n\omega\tau+w_{cn0}\cos n\omega\tau, \tag{19}$$

where $w_{cn0}=w_{cn}(0)$ and $w_{sn0}=w_{sn}(0)$.

Substituting (18) into (5) leads to:

$$\begin{aligned} &-\bar{L}_e\omega^2 y_0\sin\omega\tau+\tfrac{1}{2}c_\eta r\omega^2\left|y_0\cos\omega\tau\right|y_0\cos\omega\tau+2\bar{g}y_0\sin\omega\tau\\ &=\bar{L}_h\omega^2\sum_{n=1}^{\infty} n^2\left(w_{sn}(1)\sin n\omega\tau+w_{cn}(1)\cos n\omega\tau\right). \end{aligned} \tag{20}$$

Multiplying Eq. (20) by $\sin(n\omega\tau)$ and integrating it from 0 to the period T, $2\pi/\omega$, leads to:

$$w_{sn}(1)=\begin{cases} 0, & n\neq 1\\ \frac{1-k_d^2}{r_{he}}y_0, & n=1 \end{cases}, \tag{21}$$

where $k_d=\omega/\omega_d$ and $r_{he}=\bar{L}_h/\bar{L}_e$.

Similarly, multiplying Eq. (20) by $\cos(n\omega\tau)$ and integrating it from 0 to the period T, $2\pi/\omega$, leads to:

$$w_{cn}(1)=\begin{cases} 0,\ n=2m,\ m=1,2,3\\ \frac{(-1)^{m+1}4c_\eta r y_0^2}{(n^2-4)n^3\pi\bar{L}_h},\ n=2m+1,\ m=0,1,2,3 \end{cases}. \tag{22}$$

Substituting Eqs. (21) and (22) into Eq. (19) leads to:

$$w_{d1}(1)=y_0\sqrt{y_0^2\left[\frac{4c_\eta r}{3\pi\bar{L}_h}\right]^2+\left[\frac{\left(1-k_d^2\right)}{r_{he}k_d^2}\right]^2}, \tag{23a}$$

$$w_{q(2m)}(1)=0, \tag{23b}$$

$$w_{d(2m+1)}(1)=\frac{(-1)^{m+1}4}{n^3(n^2-4)}\frac{c_\eta r y_0^2}{\pi\bar{L}_h},\ m=1,2,3,\ldots \tag{23c}$$

Substituting Eq. (18) into governing equation (12) and using the orthogonality condition of trigonometric functions, $\{\sin(n\omega t),\ \cos(n\omega t)\}$, leads to:

$$\frac{d^4 w_{cn}}{d\xi^4}-n^2\omega^2 w_{cn}=0 \tag{24}$$

and

$$\frac{d^4 w_{sn}}{d\xi^4}-n^2\omega^2 w_{sn}=0. \tag{25}$$

Similarly, the boundary conditions (13)–(16) become:
at $\xi=0$:

$$\frac{dw_{cn}(0)}{d\xi}=0, \tag{26}$$

$$\frac{dw_{sn}(0)}{d\xi} = 0, \tag{27}$$

$$w_{cn}(0) = f_{cn}, \tag{28}$$

$$w_{sn}(0) = f_{sn}, \tag{29}$$

at $\xi = 1$:

$$\frac{d^2 w_{cn}(1)}{d\xi^2} = 0, \tag{30}$$

$$\frac{d^2 w_{sn}(1)}{d\xi^2} = 0, \tag{31}$$

$$\frac{d^3 w_{cn}(1)}{d\xi^3} + n^2\omega^2 m_{TLCD} w_{cn}(1) = 0, n = 1, 2, 3, \ldots \tag{32}$$

$$\frac{d^3 w_{sn}(1)}{d\xi^3} + n^2\omega^2 m_{TLCD} w_{sn}(1) = -\delta_{1n}\omega^2 m_h r y_0, \tag{33}$$

where

$$\delta_{1n} = \begin{cases} 1, & n = 1 \\ 0, & n \neq 1 \end{cases}.$$

So far, two independent subsystems in terms of w_{cn} or w_{sn} are found. The first subsystem in terms of w_{cn} only is composed of the transformed governing equation (24) and the boundary conditions (26, 28, 30, 32). On the other hand, the second subsystem in terms of w_{cn} only is composed of the transformed governing equation (25) and the corresponding boundary conditions (27, 29, 31, 33).

3.2. *Solution of the first subsystem*

The general solution of Eq. (24) is expressed as:

$$w_{cn}(\xi) = c_{cn1} v_{cn1}(\xi) + c_{cn2} v_{cn2}(\xi) + c_{cn3} v_{cn3}(\xi) + c_{cn4} v_{cn4}(\xi), \tag{34}$$

where the four linearly independent fundamental solutions of Eq. (24) are:

$$\begin{aligned} v_{cn1}(\xi) &= \frac{1}{2}\left[\cosh\sqrt{n\omega}\xi + \cos\sqrt{n\omega}\xi\right], \\ v_{cn2}(\xi) &= \frac{1}{2\sqrt{n\omega}}\left[\sinh\sqrt{n\omega}\xi + \sin\sqrt{n\omega}\xi\right], \\ v_{cn3}(\xi) &= \frac{1}{2n\omega}\left[\cosh\sqrt{n\omega}\xi - \cos\sqrt{n\omega}\xi\right], \\ v_{cn4}(\xi) &= \frac{1}{2(n\omega)^{3/2}}\left[\sinh\sqrt{n\omega}\xi - \sin\sqrt{n\omega}\xi\right], \end{aligned} \tag{35}$$

which satisfy the following normalized condition:

$$\begin{bmatrix} v_{i1} & v_{i2} & v_{i3} & v_{i4} \\ v'_{i1} & v'_{i2} & v'_{i3} & v'_{i4} \\ v''_{i1} & v''_{i2} & v''_{i3} & v''_{i4} \\ v'''_{i1} & v'''_{i2} & v'''_{i3} & v'''_{i4} \end{bmatrix}_{\substack{\xi=0 \\ i=cn}} = \begin{bmatrix} 1 & 0 & 0 & 0 \\ 0 & 1 & 0 & 0 \\ 0 & 0 & 1 & 0 \\ 0 & 0 & 0 & 1 \end{bmatrix}. \tag{36}$$

Substituting the solution (34) into the boundary conditions (26, 28, 30, 32), the coefficients are obtained:

$$c_{cn1} = w_{cn0} = \frac{w_{cn}(1)}{v_{cn1}(1) + \beta_{cn3} v_{cn3}(1) + \beta_{cn4} v_{cn4}(1)},$$

$$c_{cn2} = 0, \; c_{cn3} = \beta_{cn3} f_{cn},$$

$$c_{cn4} = \frac{-1}{v''_{cn4}(1)}\left(f_{cn} v''_{cn1}(1) + c_{cn3} v''_{cn3}(1)\right), \tag{37a}$$

where

$$\begin{aligned} \beta_{cn4} &= \frac{-1}{v''_{cn4}(1)}\left(v''_{cn1}(1) + \beta_{cn3} v''_{cn3}(1)\right), \\ \beta_{cn3} &= \frac{\alpha_{cn4}\frac{v''_{cn1}(1)}{v''_{cn4}(1)} - \alpha_{cn1}}{\alpha_{cn3} - \alpha_{cn4}\frac{v''_{cn3}(1)}{v''_{cn4}(1)}}, \\ \alpha_{cni} &= v'''_{cni}(1) + n^2\omega^2 m_{TLCD} v_{cni}(1). \end{aligned} \tag{37b}$$

3.3. *Solution of the second subsystem*

The general solution of Eq. (25) is expressed as:

$$w_{sn}(\xi) = c_{sn1} v_{sn1}(\xi) + c_{sn2} v_{sn2}(\xi) + c_{sn3} v_{sn3}(\xi) + c_{sn4} v_{sn4}(\xi), \tag{38}$$

where $v_{sn}i(\xi)$, $i = 1, 2, 3, 4$ are the four linearly independent fundamental solutions of Eq. (25) and $v_{sni}(\xi) = v_{cni}(\xi)$, $i = 1, 2, 3, 4$.

Substituting the solution (38) into the boundary conditions (27, 29, 31, 33), the coefficents are obtained:

$$c_{sn1} = w_{sn0} = \frac{w_{sn}(1) - \left[\frac{v''_{sn3}(1)}{v''_{sn4}(1)} v_{sn4}(1) - v_{sn3}(1)\right]\chi_{sn3}}{v_{sn1}(1) + \beta_{sn3} v_{sn3}(1) + \beta_{sn4} v_{sn4}(1)},$$

$$c_{sn2} = 0, \; c_{sn3} = \beta_{sn3} f_{sn} - \chi_{sn3},$$

$$c_{sn4} = \beta_{sn4} f_{sn} + \frac{v''_{sn3}(1)}{v''_{sn4}(1)}\chi_{sn3}, \tag{39a}$$

where

$$\beta_{sn4} = \frac{-1}{v''_{sn4}(1)}\left(v''_{sn1}(1) + \beta_{sn3} v''_{sn3}(1)\right), \beta_{sn3} = \frac{\alpha_{sn4}\frac{v''_{sn1}(1)}{v''_{sn4}(1)} - \alpha_{sn1}}{\alpha_{sn3} - \alpha_{sn4}\frac{v''_{sn3}(1)}{v''_{sn4}(1)}},$$

$$\chi_{sn3} = \frac{\delta_{1n}\omega^2 m_h r y_0}{\alpha_{sn3} - \alpha_{sn4}\frac{v''_{sn3}(1)}{v''_{sn4}(1)}}, \alpha_{sni} = v'''_{sni}(1) + n^2\omega^2 m_{TLCD} v_{sni}(1). \tag{39b}$$

Substituting the coefficients (37, 39) into Eqs. (34), (38), and (18), the dynamic displacement of the beam is determined.

4. Numerical results and discussion

In general, the liquid of TLCD flows through the orifice induces the energy dissipation and effect of damping for the structure. The larger the flow velocity through the orifice is, the greater the energy dissipation. Obviously, it is the target of the design of TLCD for suppression of vibration that the larger liquid motion and smaller displacement of structure are preferred. This study starts with the investigation of the nonlinear dynamic behavior of TLCD based on Eq. (23). It is observed that if ω approaches to zero, $w_{d1}(1)$ becomes infinite. It means that the damping effect of TLCD is negligible. Moreover, $w_{d1}(1)$ depends on the frequencies of excitation and TLCD, but $w_{dn}(1)$, $n = 2, 3, \ldots$, not. Further, Eq. (23) leads to the gradient of the response

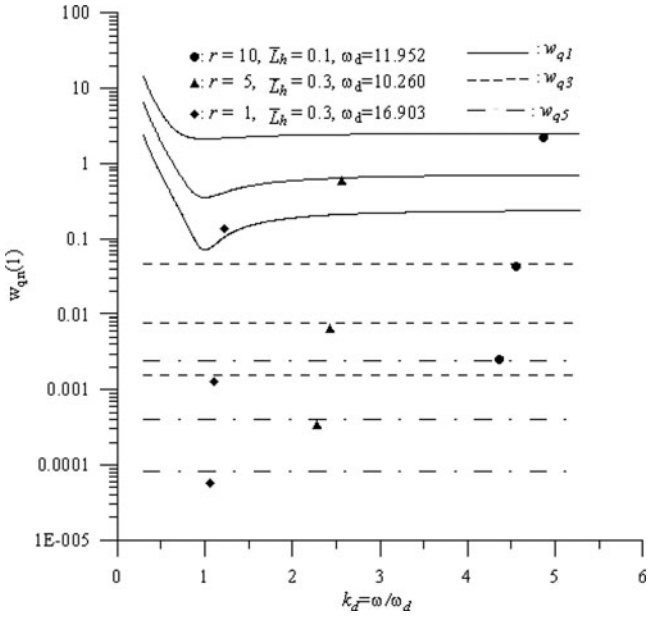

Figure 2. Relation between the frequency ratio k_d and the tip displacements of the structure with TLCD. [$\bar{g} = 100$, $\bar{L}_v = 0.2$, $y_0 = 0.1$, $c_\eta = 5$.]

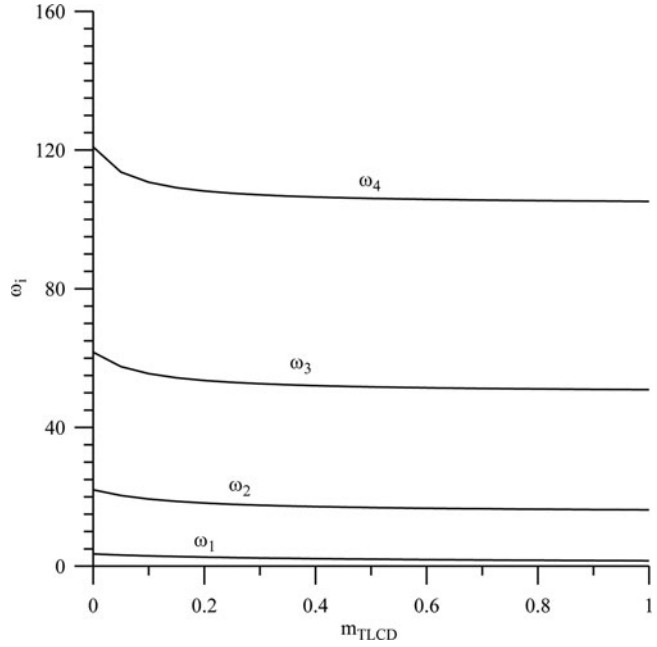

Figure 3. Natural frequencies of a cantilever with tip mass.

ratio:

$$\frac{\partial}{\partial k_d}\left(\frac{w\,(1,\tau)}{y_0}\right) = \frac{-2\left(1-k_d^2\right)}{r_{he}^2 k_d^5 \sqrt{\left[y_0^2\left[\frac{4c_\eta r}{3\pi \bar{L}_h}\right]^2 + \left[\frac{\left(1-k_d^2\right)}{r_{he}k_d^2}\right]^2\right]}} \sin\left(\omega\tau + \theta_1\right). \quad (40)$$

Equation (40) reveals that if k_d is equal to the unit, the amplitude of $\left|w\,(1,\tau)\,/y_0\right|$ is zero. In other words, under this condition the damping effect of TLCD is optimal. In addition to the frequency ratio several parameters affect the response ratio. It is numerically demonstrated in Figure 2. It verifies that if the ratio of the excitation frequency to the TLCD one, $k_d = \omega/\omega_d$, is equal to the unit, the response ratio of the tip displacement to the liquid amplitude, $w_{q1}\,(1)\,/y_0$ is the minimum. The response ratio of the case with $\{r = 1, \bar{L}_h = 0.3, \omega_d = 16.903\}$ is 0.06. It implies that if $k_d = 1$ and with these parameters, the suppression of vibration is effective. However, the response ratios of the cases with $\{r = 5, \bar{L}_h = 0.3, \omega_d = 10.260\}$ and $\{r = 10, \bar{L}_h = 0.1, \omega_d = 11.952\}$ are 0.35 and 2.3, respectively. Obviously, these conflict the above requirements for suppressing structural vibration. Moreover, it is found that the larger the area ratio, $r = A_v/A_h$, of TLCD is the larger the response ratio. In other words, the area ratio r should not be too larger. Moreover, Figure 2 demonstrates that the first term w_{d1} of the tip displacement (Eq. 18) dominates. The even terms are zero. Moreover, the amplitude of the higher term is considerably gradually smaller.

Obviously, the relation between the natural frequencies of the tall building and the TLCD is important for the vibration suppression. In addition to the performance of TLCD, investigating the behavior of the tall building is helpful for the vibration suppression. Here the building with TLCD can be simulated as a cantilever beam with a tip mass. The frequency equation is derived and listed in Appendix C. Further, the influence of the tip mass on the natural frequencies is shown in Figure 3.

Figures 4a, 4b, and 4c demonstrate the effect of c_η and the excitation frequency ω on the vibration spectrum of the structure with TLCD. The natural frequency of TLCD is assumed to be the same as the first natural one of the beam with TLCD, which the attached mass is considered as a concentrated mass. The first three exact dimensionless natural frequencies $\{\omega_{n1}, \omega_{n2}, \omega_{n3}\}$ are {2.9678, 19.3558, 55.5182}. It is observed from Figure 4a with $\omega_d = \omega_{n1}$ that when the damping coefficient c_η is very small, i.e., slight damping effect, two natural frequencies take place of the first original one of a beam with a concentrated mass. It is because the relative motion of the liquid generates the additional vibration modes. Moreover, this phenomenon is proved theoretically here. Equation (22) shows that if the TLCD damping coefficient approaches to zero, the coefficient $w_{cn}(1)$ becomes negligible. The motion of the top end of beam is dominated by $w_{sn}(1)$. Further, Eq. (21) demonstrates that if $k_d = \omega/\omega_d$ is less or more than the unit, the direction of $w_{sn}(1)$ is same as that of liquid in TLCD or reverse. Therefore, there exist two different motions close to the original natural frequency and two resonant spectrums, as shown in Figure 4a. Moreover, it is revealed from Eq. (23) that if the damping coefficient is zero, the tip displacement becomes:

$$w\,(1,\tau) = y_0 \frac{\left(1-k_d^2\right)}{r_{he}k_d^2} \sin\left(\omega\tau + \pi/2\right). \quad (41)$$

Further, if the frequency ratio k_d is unit, the tip displacement becomes zero. In other words, if the natural frequency of TLCD without the damping effect is the same as that of the building, the vibration of building can be completely suppressed. However, at two frequency ratios near the unit there exist infinite the response ratio. The useful range of operation for vibration suppression is too narrow. When the damping coefficient is increased, the phenomenon of complete suppression disappears. However, the useful range of operation is extended. It has been verified in Figure 4a. This behavior is like that of 2DOF model [16].

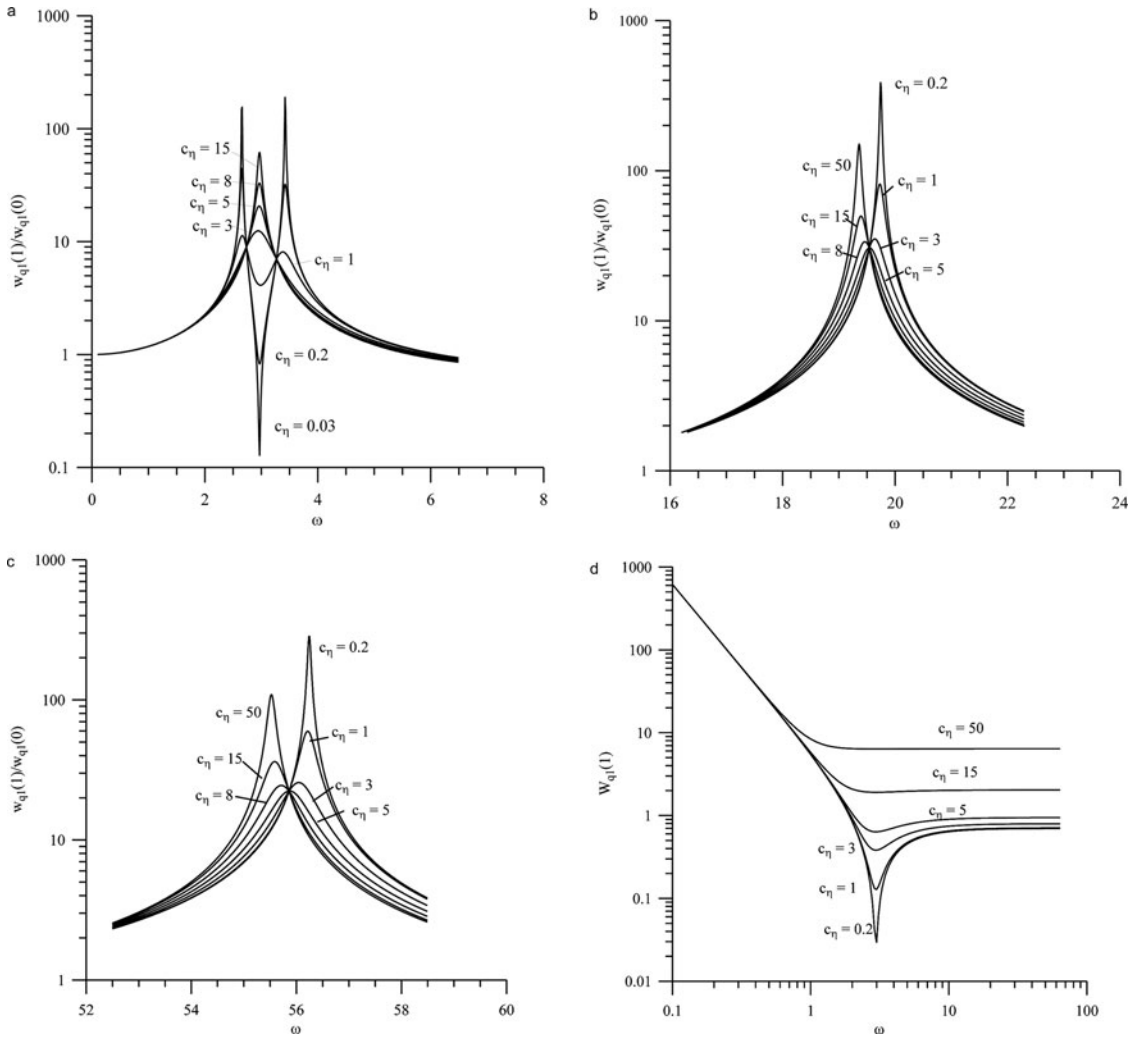

Figure 4. Influence of the damping coefficient c_η and the excitation frequency ω on the vibration spectrum of the structure with TLCD: (a) Frequency spectrum close to the first frequency of the beam with the fixed concentrated mass. (b) Frequency spectrum close to the second frequency of the beam with the fixed concentrated mass. (c) Frequency spectrum close to the third frequency of the beam with the fixed concentrated mass. (d) Response wq1(1) of TLCD. [$\bar{g} = 3.0827, \bar{L}_h = 0.1, \bar{L}_v = 0.2, m_h = 0.05, m_{TLCD} = 0.1, r = 3, y_0 = 0.1, \omega_d = \omega_{n1} = 2.9678$.]

It is observed from Eq. (22) that $w_{cn}(1)$ changes with the damping coefficient c_η. The larger the damping coefficient c_η is, the more the tip displacement $w_{cn}(1)$. In other words, if the damping coefficient c_η is too large, the resonant response becomes larger. The physical reason is that increasing the damping coefficient means decreasing the hole size of the orifice and increasing the flow resistance through the orifice. When damping coefficient is very large, almost no liquid flows through the orifice. As shown in Figure 4a, the resonance happens as $c_\eta > 15$. The TLCD is like a rigid concentrated mass. It should be noted that Wu et al. [10] proposed that the best damping coefficient $c_\eta = 5$ is for the structural control of bridge pitching motion. However, for the structural control of building transverse motion the best parameter is about $c_\eta = 2$.

Figure 4b demonstrates the frequency spectrum close to the second frequency of the beam with the fixed concentrated mass. Its exact frequency is 19.3558. The corresponding tip displacement $w_{sn}(1)$ of Eq. (21) is almost independent to the excitation frequency if this frequency is large enough. Therefore, it does not happen that two natural frequencies take place of the second original one, as shown in Figure 4a. The theoretical description is from Eq. (22) that if the TLCD damping coefficient approaches to zero, the coefficient $w_{cn}(1)$ becomes negligible. The motion of the top end of the beam is dominated by $w_{sn}(1)$. Moreover, Eq. (21) demonstrates that if $k_d >> 1$, $w_{sn}(1)$ is negative only. Further, increasing the damping coefficient c_η from zero depresses obviously the vibration response. However, for $c_\eta > 5$, the larger the damping coefficient c_η is, the greater the vibration response. It is because $w_{cn}(1)$ changes with the damping coefficient c_η and the dissipation effect of TLCD disappears.

Figure 4c demonstrates the frequency spectrum close to the third frequency of the beam with the fixed concentrated mass. The third exact frequency is 55.5182. The performance is like Figure 4b. Moreover, although the natural frequency of TLCD is inconsistent to that of beam, the TLCD is helpful for the anti-vibration of the higher-mode.

Figure 4d with $y_0 = 0.1$ shows that if $k_d = 1$, the smaller the damping coefficient is, the smaller the response ratio $w_{q1}(1)$ of the TLCD. As shown in Figure 4a, at $k_d = 1$, the response ratio is very small, but there are two resonant responses close to the first original natural frequency happening. Moreover, if $c_\eta > 5$,

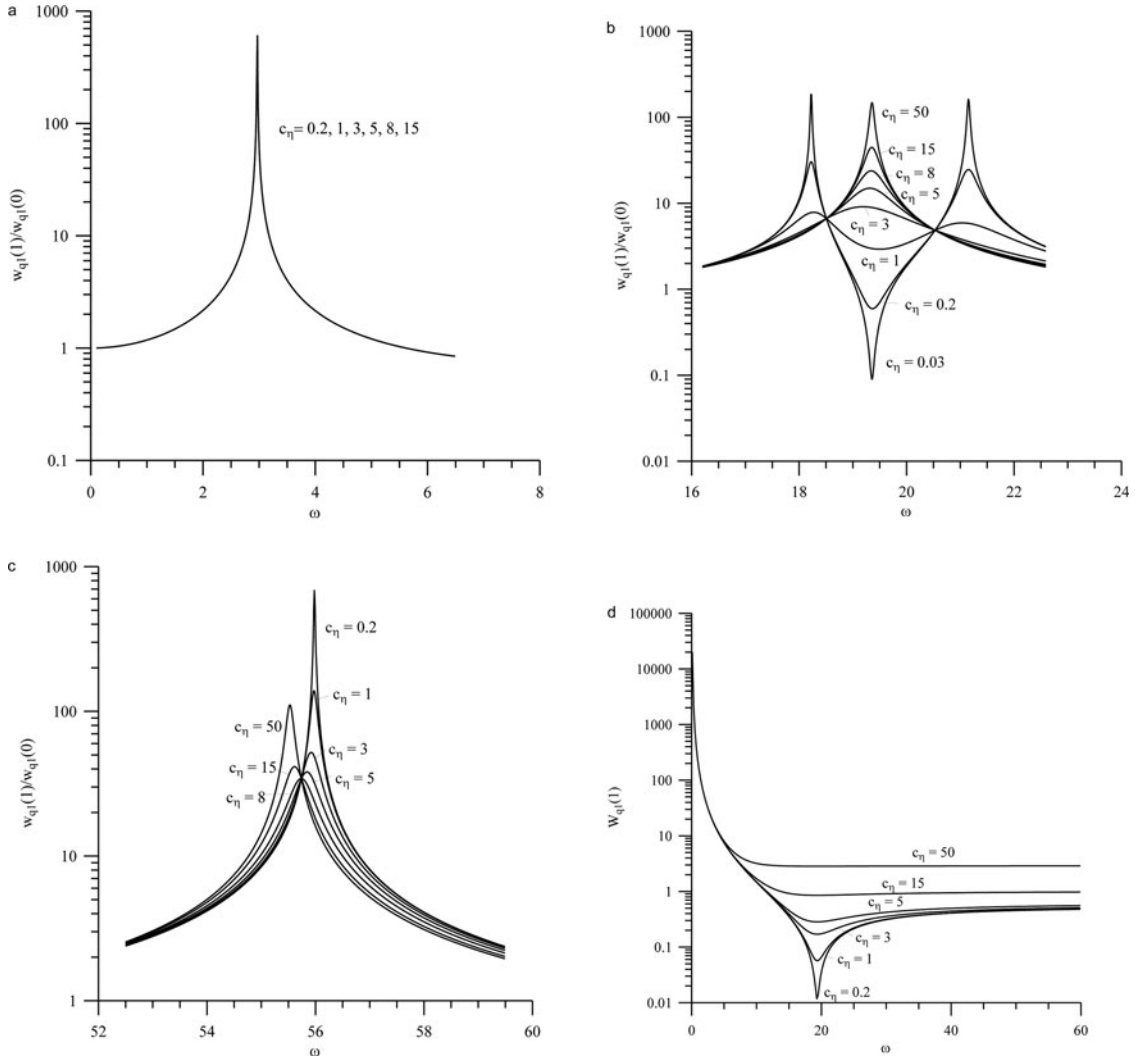

Figure 5. Influence of the damping coefficient c_η and the excitation frequency ω on the vibration spectrum of the structure with TLCD: (a) Frequency spectrum close to the first frequency of the beam with the fixed concentrated mass. (b) Frequency spectrum close to the second frequency of the beam with the fixed concentrated mass. (c) Frequency spectrum close to the third frequency of the beam with the fixed concentrated mass. (d) Response wq1(1) of TLCD. [$\bar{g} = 100, \bar{L}_h = 0.1, \bar{L}_v = 0.2, m_h = 0.05, m_{TLCD} = 0.1, r = 1.3383, y_0 = 0.1, \omega_d = \omega_{n2} = 19.3558$.]

the response ratio w_{q1}/y_0 is too large. No damping effect on the structural control exists.

Figures 5a, 5b, and 5c demonstrate the frequency spectrums of the beam with TLCD close to the first three natural frequencies of the beam with the fixed concentrated mass. The natural frequency of TLCD is the same as the second natural frequency, $\omega_d = \omega_{n2} = 19.3558$. Figure 5a shows that the effect of the damping coefficient on the first resonant response is negligible. The TLCD is not helpful for the anti-vibration of the first mode. This is greatly different to the above case. The reason is demonstrated in Figure 5d that if $\omega < \omega_d$, no matter what the damping coefficient c_η is, the response ratio w_{q1}/y_0 is too large. In other words, no damping effect on the structural control exists.

It is observed from Figure 4b with $\omega_d = \omega_{n2}$ that when the damping coefficient c_η is very small, two natural frequencies take place of the second original one of a beam with a concentrated mass. It is because the relative motion of the liquid generates the additional vibration modes. This phenomenon is like Figure 4a. Increasing this damping coefficient from zero decreases the response ratio. When $c_\eta = 1$, the response ratio is small. If $c_\eta > 3$, the resonant frequency is obviously increased. Moreover, the more the damping coefficient c_η is, the larger the response ratio.

Similarly, Figure 5c demonstrates that increasing this coefficient from zero decreases the response ratio. When $c_\eta = 8$, the response ratio is almost the minimum. If $c_\eta > 8$, the resonant frequency is decreased slightly. If $c_\eta > 8$, the more the damping coefficient c_η is, the larger the response ratio.

Figure 6 demonstrates the frequency spectrums of the beam with TLCD. The natural frequency of TLCD is the same as the natural frequency, $\omega_d = \omega_{n3} = 55.5182$. Figures 6a and 6b show that the effect of the damping coefficient on the first two resonant responses is negligible. The TLCD is not helpful for the anti-vibration of the first two modes. The reason is found from Figure 6d that if $\omega < \omega_d$, in spite of the damping coefficient c_η the response ratio w_{q1}/y_0 is very large.

Similarly, it is observed from Figure 6c that when $\omega \to \omega_{n3}$ and the damping coefficient c_η is very small, two natural frequencies take place of the third original one of a beam with a

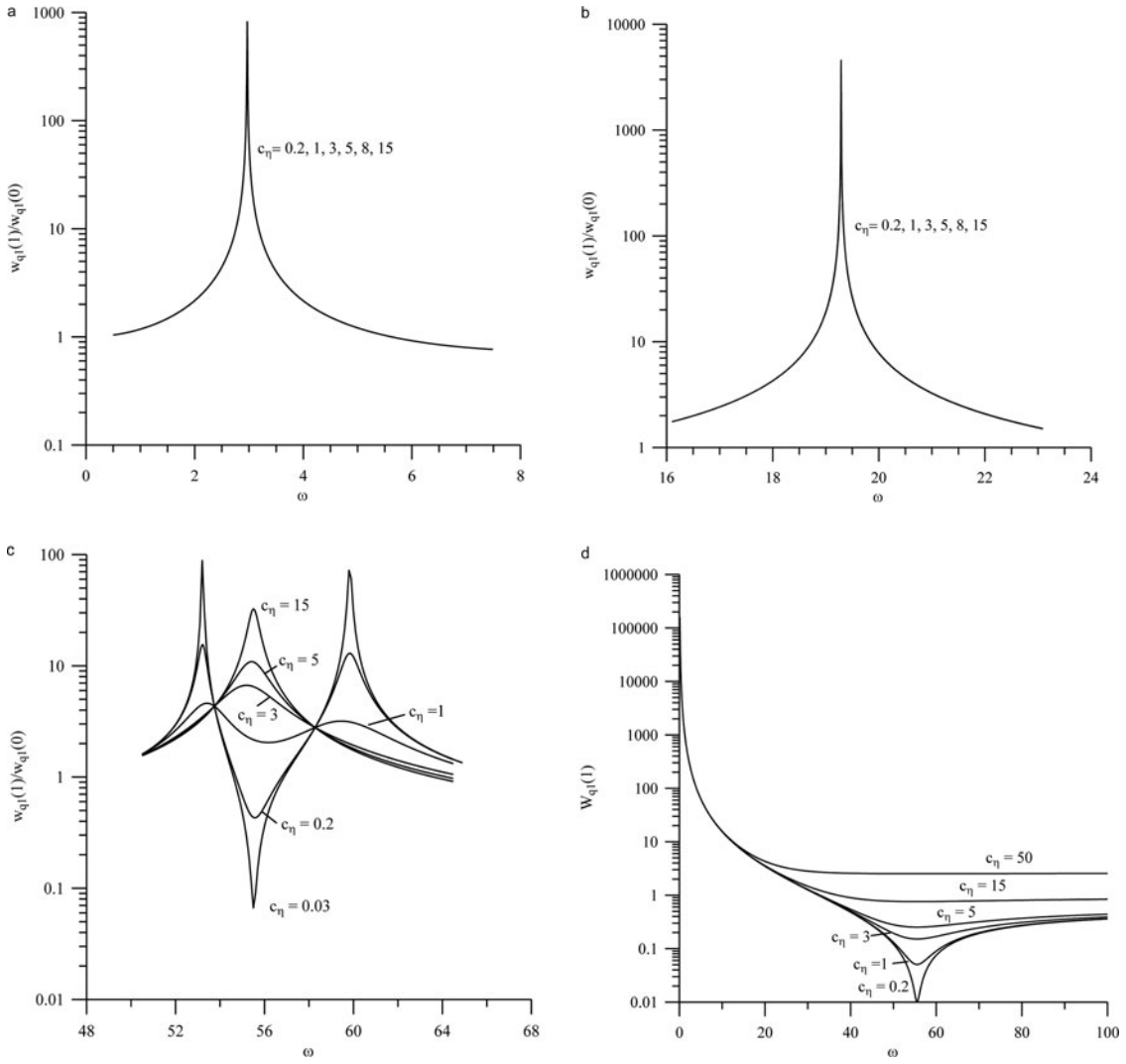

Figure 6. Influence of the damping coefficient c_η and the excitation frequency ω on the vibration spectrum of the structure with TLCD: (a) Frequency spectrum close to the first frequency of the beam with the fixed concentrated mass. (b) Frequency spectrum close to the second frequency of the beam with the fixed concentrated mass. (c) Frequency spectrum close to the third frequency of the beam with the fixed concentrated mass. (d) Response wq1(1) of TLCD. [$\bar{g} = 800$, $\bar{L}_h = 0.1$, $\bar{L}_v = 0.2$, $m_h = 0.05$, $m_{TLCD} = 0.1$, $r = 1.191$, $y_0 = 0.1$, $\omega_d = \omega_{n3} = 55.5182$.]

concentrated mass. This phenomenon is like Figures 4a and 5b. If $c_\eta > 3$, the more the damping coefficient c_η is, the larger the response ratio.

Based on the above discussion, it is found that if the dimensionless natural frequencies of the TLCD and the structure are consistent, $\omega_d = \omega_i$, the effective vibration suppression will be established. It means that the optimum dimensions of the TLCD can be designed for arbitrary building. For example, if the bending rigidity EI, the mass per unit length ρA, and the height L of the building are arbitrarily given, the corresponding optimum effective length of TLCD can be directly determined via:

$$L_e = \frac{2g\rho A L^4}{\omega_i^2 EI}, \tag{42}$$

where ω_i are the dimensionless natural frequencies. For a uniform tall building in Figure 4, its first three dimensionless natural frequencies $\{\omega_1, \omega_2, \omega_3\}$ are {2.9678, 19.3558, 55.5182}. Obviously, the results in terms of dimensionless parameters can be easily and generally applied to any real case just by giving the real material and geometry properties. Moreover, it reveals that the effective length L_e decreases with higher dimensionless natural frequency ω and bending rigidity EI. However, it increases with the mass per unit length ρA and the height of building L.

5. Conclusion

In this study, the nonlinear vibration control of a tall structure with TLCD is investigated. The analytical solution of this model is presented. It is found that if the natural frequency of TLCD is close to that of the structure, the TLCD can suppress effectively the resonant responses. Moreover, the following phenomena are revealed:

(1) If the frequency of liquid oscillation ω approaches to zero, the damping effect of TLCD is negligible.
(2) If the frequency of liquid oscillation ω is smaller than the natural frequency of TLCD ω_d, no matter what the damping coefficient c_η is, the damping effect on the structural control is negligible.
(3) For successful vibration, suppressing the effective length L_e is recommended as the relation [39]. It decreases with

the frequency of liquid oscillation ω and bending rigidity EI and increases with the mass per unit length ρA and the height of building L.

(4) If the area of the horizontal channel of TLCD is reduced, as shown in Figure 1c, the effective length L_e is increased and its natural frequency is decreased.

(5) If the horizontal channel is in series connection, as shown in Figure 1d, the effective length L_e is greatly increased and the natural frequency of TLCD is decreased significantly.

(6) If the natural frequency of TLCD without the damping effect is the same as that of the building, the vibration of the building can be completely suppressed. However, the useful range of operation for vibration suppression is very narrow. Therefore, the damping effect must be considered for extending the useful range although the tip vibration cannot be controlled to zero.

Funding

The support of the National Science Council of Taiwan, R. O. C., is gratefully acknowledged (Grant number: Nsc99-2221-E168-020).

References

[1] J.F. Wang and C.C. Lin, Seismic performance of multiple tuned mass dampers for soil–irregular building interaction systems, Int. J. Solids Struct., vol. 42, pp. 5536–5554, 2005.

[2] M.Y. Liu, W.L. Chiang, J.H. Hwang, and C.R. Chu, Wind-induced vibration of high-rise building with tuned mass damper including soil–structure interaction, J. Wind Eng. Ind. Aerodyn., vol. 96, pp. 1092–1102, 2008.

[3] M. Matsui and Y. Tamura, Development of a hybrid vibration experiment system for determining wind-induced responses of buildings with tuned dampers, J. Wind Eng. Ind. Aerodyn., vol. 96, pp. 2033–2041, 2008.

[4] T. Balendra, C.M. Wang, and G. Rakesh, Vibration control of various types of buildings using TLCD, J. Wind Eng. Ind. Aerodyn., vol. 83, pp. 197–208, 1999.

[5] C.C. Lin, J.M. Ueng, and T.C. Huang, Seismic response reduction of irregular buildings using passive tuned mass dampers, Eng. Struct., vol. 22, pp. 513–524, 1999.

[6] C.C. Lin, J.F. Wang, and J.M. Ueng, Vibration control identification of seismically excited M.D.O.F. structure—PTMD systems, J. Sound Vib., vol. 240, pp. 87–115, 2001.

[7] K. Shankar and T. Balendra, Application of the energy flow method to vibration control of buildings with multiple tuned liquid dampers, J. Wind Eng. Ind. Aerodyn., vol. 90, pp. 1893–1906, 2002.

[8] J.Y. Wang, Y.Q. Ni, J.M. Ko, and B.F. Spencer Jr., Magneto-rheological tuned liquid column dampers (MR-TLCDs) for vibration mitigation of tall buildings: Modelling and analysis of open-loop control, Comput. Struct., vol. 83, pp. 2023–2034, 2005.

[9] K.M. Shum, Closed form optimal solution of a tuned liquid column damper for suppressing harmonic vibration of structures, Eng. Struct., vol. 31, pp. 84–92, 2009.

[10] J.C. Wu, Y.P. Wang, C.L. Lee, P.H. Liao, and Y.H. Chen, Wind-induced interaction of a non-uniform tuned liquid column damper and a structure in pitching motion, Eng. Struct., vol. 30, pp. 3555–3565, 2008.

[11] S. Colwell and B. Basu, Tuned liquid column dampers in offshore wind turbines for structural control, Eng. Struct., vol. 31, pp. 358–368, 2009.

[12] R. Debbarma, S. Chakraborty, and S.K. Ghosh, Optimum design of tuned liquid column dampers under stochastic earthquake load considering uncertain bounded system parameters, Int. J. Mech. Sci., vol. 52, pp. 1385–1393, 2010.

[13] S.K. Lee, K.W. Min, and H.R. Lee, Parameter identification of new bidirectional tuned liquid column and sloshing dampers, J. Sound Vib., vol. 28, pp. 1312–1327, 2011.

[14] T. Balendra, C.M. Wang, and H.F. Cheong, Effectiveness of tuned liquid column dampers for vibration control of towers, Eng. Struct., vol. 17, no. 9, pp. 668–675, 1995.

[15] J.C. Wu, C.H. Chang, and Y.Y. Lin, Optimal designs for non-uniform tuned liquid column dampers in horizontal motion, J. Sound Vib., vol. 326, pp. 104–122, 2009.

[16] D.J. Inman, Engineering Vibration, Prentice Hall International, Upper Saddle River, NJ, 1996.

Appendix A

The derivation of equation of motion of TLCD is shown in Figure 1c. Some area of the horizontal channel is closed.

Lagrange's equation is:

$$\frac{\partial}{\partial t}\left(\frac{\partial\,(T-V)}{\partial \dot{y}}\right)-\frac{\partial\,(T-V)}{\partial y}=Q_y, \tag{A1}$$

where the kinetic energy includes:

$$T=T_{left}+T_{right}+T_{hopen}+T_{hclosed}. \tag{A2}$$

In which the kinetic energies in the left and right vertical columns are:

$$T_{left}=\frac{1}{2}\rho\left(L_v-y\right)A_v\left(\dot{y}^2+\dot{x}^2\right), T_{right}=\frac{1}{2}\rho\left(L_v+y\right)A_v\left(\dot{y}^2+\dot{x}^2\right). \tag{A3}$$

The kinetic energies in the open and closed horizontal channels are:

$$T_{hopen}=\frac{1}{2}\rho A_{hopen}L_h\left(\dot{x}+r_{open}\dot{y}\right)^2, T_{hclosed}=\frac{1}{2}\rho A_{hclosed}L_h\dot{x}^2. \tag{A4}$$

The potential energy is:

$$V=\rho g A_v\frac{1}{2}\left(L_v-y\right)^2+\rho g A_v\frac{1}{2}\left(L_v+y\right)^2. \tag{A5}$$

The damping force is:

$$Q_y=-\frac{1}{2}\rho r_{open}\dot{y}\left|r_{open}\dot{y}\right|c_\eta A_{hopen}, \tag{A6}$$

in which

$$r_{open}=\frac{A_v}{A_{hopen}}. \tag{A7}$$

Substituting Eqs. (A2)–(A6) into Eq. (A1) and defining $r=r_{open}$ and $L_e=L_v+r_{open}L_h$, the equation of motion as Eq. (1) is obtained.

Appendix B

The derivation of equation of motion of TLCD is shown in Figure 1d. The horizontal channel is in series connection.

Lagrange's equation is:

$$\frac{\partial}{\partial t}\left(\frac{\partial\,(T-V)}{\partial \dot{y}}\right)-\frac{\partial\,(T-V)}{\partial y}=Q_y, \tag{B1}$$

where the kinetic energy includes:

$$T = T_{left} + T_{right} + T_{hf} + T_{hb}, \tag{B2}$$

in which the kinetic energies in the left and right vertical columns are the same as those of (A3). The kinetic energy of the horizontal column includes the forward and backward parts:

$$T_{hf} = \frac{1}{2}\rho A_{Hs} L_{HF}\left(\dot{x} + r_s\dot{y}\right)^2, \; T_{hb} = \frac{1}{2}\rho A_{Hs} L_{HB}\left(\dot{x} - r_s\dot{y}\right)^2, \tag{B3}$$

in which L_{HF} and L_{HB} are the lengths of the forward and backward parts, respectively.

$$r_s = \frac{A_v}{A_{Hs}}. \tag{B4}$$

The potential energy is the same as Eq. (A5). The damping force is:

$$Q_y = -\frac{1}{2}\rho r_s\dot{y}\left|r_s\dot{y}\right| c_\eta A_{hs}. \tag{B5}$$

Substituting Eqs. (B2)–(B5) into Eq. (B1) and defining $r = r_s, L_h = L_{HF} - L_{HB}, A_h = A_{Hs}$, and $L_e = 2L_v + (L_{HF} + L_{HB})\, r_s$, the equation of motion as Eq. (1) is obtained.

Appendix C

The natural frequency of a cantilever with tip mass is determined as follows:

The dimensionless governing differential equation of a uniform beam is:

$$\frac{\partial^4 w}{\partial\xi^4} + \frac{\partial^2 w}{\partial\tau^2} = 0, \tag{C1}$$

The boundary conditions of a cantilever with tip mass are:

at $\xi = 0$:

$$\frac{\partial w}{\partial\xi} = 0, \tag{C2}$$

$$w = 0, \tag{C3}$$

at $\xi = 1$:

$$\frac{\partial^2 w}{\partial\xi^2} = 0, \tag{C4}$$

$$-\frac{\partial^3 w}{\partial\xi^3} + m_{TLCD}\frac{\partial^2 w}{\partial\tau^2} = 0. \tag{C5}$$

The general solution of Eq. (C1) is expressed as:

$$w = \bar{w}\left(\xi\right)\sin\omega\tau. \tag{C6}$$

Substituting Eq. (C6) into Eqs. (C1)–(C5), one obtains:

$$\frac{d^4 w}{d\xi^4} - \omega^2\bar{w} = 0, \tag{C7}$$

at $\xi = 0$:

$$\frac{d\bar{w}}{d\xi} = 0, \tag{C8}$$

$$\bar{w} = 0, \tag{C9}$$

at $\xi = 1$:

$$\frac{d^2\bar{w}}{d\xi^2} = 0, \tag{C10}$$

$$\frac{d^3\bar{w}}{d\xi^3} + m_{TLCD}\omega^2\bar{w} = 0. \tag{C11}$$

The general solution of Eq. (C7) is expressed as:

$$\bar{w}\left(\xi\right) = c_1 v_1\left(\xi\right) + c_2 v_2\left(\xi\right) + c_3 v_3\left(\xi\right) + c_4 v_4\left(\xi\right), \tag{C12}$$

where the four linearly independent fundamental solutions are:

$$\begin{aligned} v_1\left(\xi\right) &= \frac{1}{2}\left[\cosh\sqrt{\omega}\xi + \cos\sqrt{\omega}\xi\right], \\ v_2\left(\xi\right) &= \frac{1}{2\sqrt{\omega}}\left[\sinh\sqrt{\omega}\xi + \sin\sqrt{\omega}\xi\right], \\ v_3\left(\xi\right) &= \frac{1}{2\omega}\left[\cosh\sqrt{\omega}\xi - \cos\sqrt{\omega}\xi\right], \\ v_4\left(\xi\right) &= \frac{1}{2\left(\omega\right)^{3/2}}\left[\sinh\sqrt{\omega}\xi - \sin\sqrt{\omega}\xi\right], \end{aligned} \tag{C13}$$

which satisfy the following normalized condition:

$$\begin{bmatrix} v_1 & v_2 & v_3 & v_4 \\ v_1' & v_2' & v_3' & v_4' \\ v_1'' & v_2'' & v_3'' & v_4'' \\ v_1''' & v_2''' & v_3''' & v_4''' \end{bmatrix}_{\xi=0} = \begin{bmatrix} 1 & 0 & 0 & 0 \\ 0 & 1 & 0 & 0 \\ 0 & 0 & 1 & 0 \\ 0 & 0 & 0 & 1 \end{bmatrix}. \tag{C14}$$

Substituting Eq. (C12) into the boundary conditions (C8)–(C11) leads to the frequency equation:

$$\left[\cosh\sqrt{\omega}\cos\sqrt{\omega} + 1\right] - m_{TLCD}\sqrt{\omega}\left[\sin\sqrt{\omega}\cosh\sqrt{\omega} - \sinh\sqrt{\omega}\cos\sqrt{\omega}\right] = 0. \tag{C15}$$